Electronic Supplementary Material (ESI) for Materials Chemistry Frontiers.

Supporting Information

Effective demulsification for oil-water separation through the metal-organic frameworks with amphipathic micro-domain

Rui Wang[a,b], Yi Feng[b], Haijuan Xu[c], Yanzhao Zou[a,b], Leiyi Fan[a,b], Ruiyang Zhang[a,b], Ying Zhou[a,b,*]

[a] State Key Laboratory of Oil and Gas Reservoir Geology and Exploitation, Southwest Petroleum University, Chengdu 610500, China

[b] The Center of New Energy Materials and Technology, School of New Energy and Materials, Southwest Petroleum University, Chengdu 610500, China

c Department of Chemistry and Environmental Engineering, Hubei Minzu University, Enshi 445000, China

* Corresponding author. Tel: +028-83037411; Fax: +86-28-83037406; E-mail: yzhou@swpu.edu.cn

Table of Content

Text S1 Methods and parameters for the characterization of material

The XRD pattern was collected by X'pert diffractometer (PANalytical, Netherlands) with an X-ray radiation of Cu *K*α (40 kV, 40 mA). The SEM image was collected by FEI Quanta430 microscope operated at 20 kV. The N_2 isothermal adsorption/desorption was carried out on Autosorb iQ station (Quantachrome Instruments, American) at 77 K with an outgas condition of 150 ℃ and 10 h. The range of relative pressure (p/p_0) was 2.05×10^{-7} ~ 9.95×10^{-1}. The specific surface area and pore size distribution were calculated by Brunauer-Emmett-Teller (BET) model, Non Local Density Functional Theory (NLDFT).

Table S1 Parameters of pore structure for the as-prepared MIL-100(Fe)

Surface special area ($m^2 \cdot g^{-1}$)	Total volume ($cm^3 \cdot g^{-1}$)	Micropore volume ($cm^3 \cdot g^{-1}$)	Internal surface special area ($m^2 \cdot g^{-1}$)	Porosity (%)
1344	0.727	0.486	1206	89.7

$$\text{Porosity (\%)} = 100 * S_i/S_s$$

Where, the S_s and S_e were the surface special area and internal surface special area.

Table S2 Comparation of dehydration time for the crude oil emulsion over different demulsifiers

	Properties of crude oil emulsion			Dehydration time	Literature
Demulsifier	Density	Viscosity	Water content		
MIL-100(Fe)	0.77 $g \cdot cm^{-3}$ (20 ℃)	13.90 $mN \cdot s \cdot m^{-1}$ (20 ℃)	90% ($v \cdot v^{-1}$)	< 5 min (RT)	In this work
AMPS-EOA/HEMA	0.896	-	50% ($v \cdot v^{-1}$)	≥ 220 min (60 ℃)	16
AMPS-EOA/HEMAP	(60 °F)			≥ 440 min (60 ℃)	16
D1	35.29	14.97 Cst (40 ℃)	30% ($v \cdot v^{-1}$)	120 min (60 ℃)	18
D2	(API, 60 °F)			> 180 min (60 ℃)	18
MJTJU-2	-	-	10% ($v \cdot v^{-1}$)	10 min (50 ℃)	35
EC	0.87 $g \cdot cm^{-3}$ (60 ℃)	15.79 $mPa \cdot s^{-1}$ (60 ℃)	30% ($v \cdot v^{-1}$)	50 min (60 ℃)	36
ECFR				10 min (60 ℃)	36

PSADP	0.962 g·cm^{-3} (25 ℃)	540 mPa·s^{-1} (65 ℃)	-	30 min (65 ℃)	37
F-MWCNTs	0.86 g·cm^{-3} (20 ℃)	8.01 mm^2·s^{-1} (50 ℃)	-	30 min (25 ℃)	38
Chitosan loaded $Ti_3C_2T_x$	-	-	≈4% (w·w^{-1})	300 min	39
FPPM	-	-	-	> 68 h (23 ℃)	40

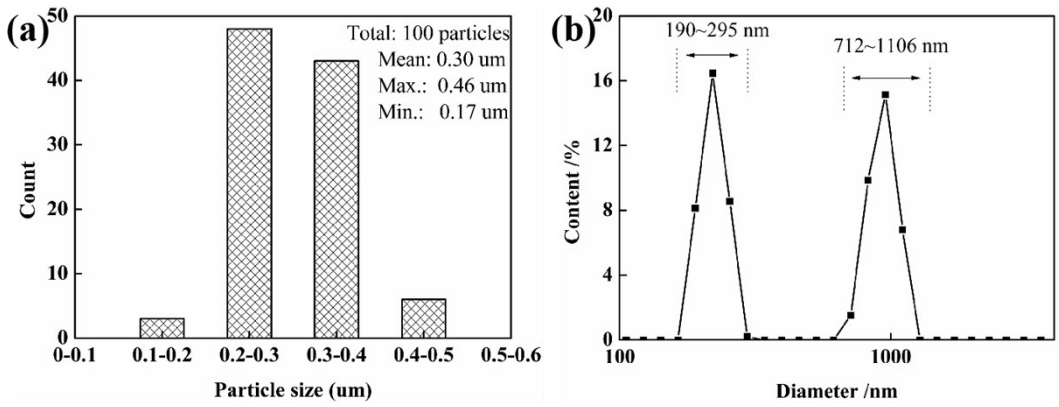

Figure S1 Statistics of particles via the result of SEM image (a), particle size distribution measured by the DLS (b) for the as-prepared MIL-100(Fe)

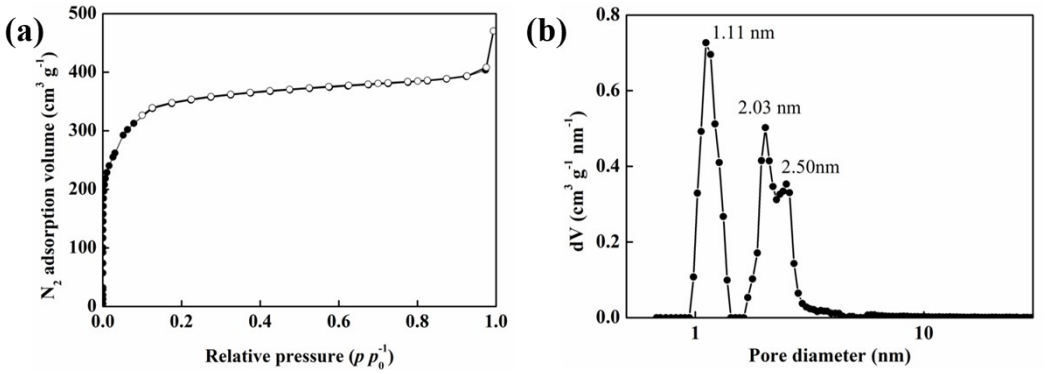

Figure S2 N_2 adsorption/desorption isotherms (a) and distribution of pore (b) for the as-prepared MIL-100(Fe)

Figure S3 Wettability of the oleic acid (a) and water (b) on the surface of the as-prepared MIL-100(Fe)

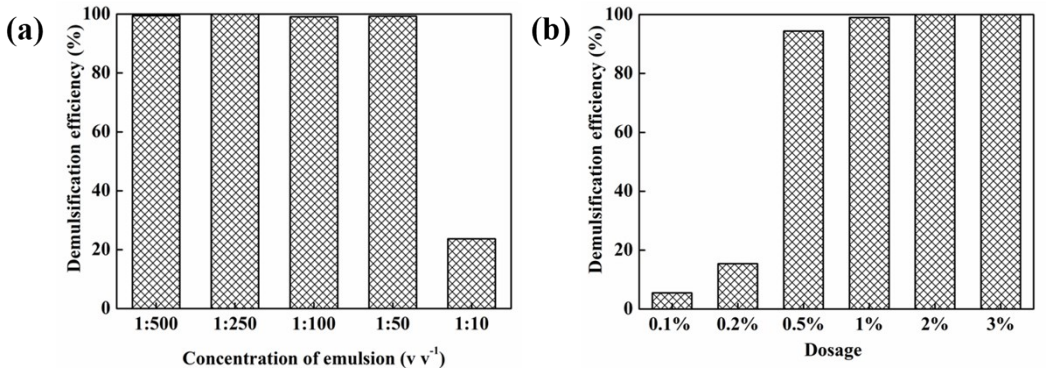

Figure S4 Demulsification efficiency for model emulsion using MIL-100(Fe) at different concentration of emulsion (a) and dosage of MIL-100(Fe) (b)

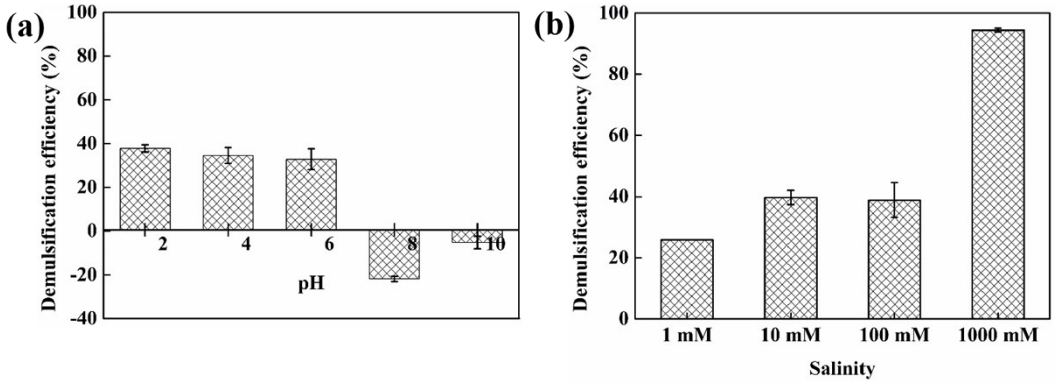

Figure S5 Control experiments about the influence of pH (a) and salinity (b) on the stability of SDS stabilized O/W model emulsion

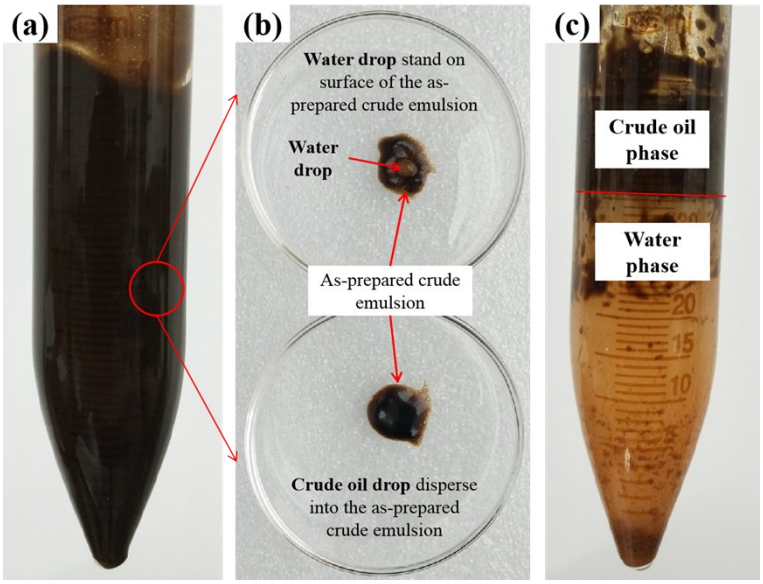

Figure S6 Optical photograph of as-prepared crude oil emulsion (a), dispersibility for the water and crude oil on the as-prepared crude emulsion (b), and dehydration of the as-prepared crude oil emulsion using MIL-100(Fe) (c)

The as-prepared crude oil emulsion was dropped on the glass surface, then the water and crude oil were dropped on the as-prepared crude oil emulsion, respectively. It was found that the water drop stood on the surface of as-prepared crude oil emulsion, while the crude oil permeated into the as-prepared crude oil emulsion quickly as shown in **Figure S5b**, indicating the external phase of the as-prepared crude oil emulsion

was crude oil. This result suggested that the as-prepared crude oil emulsion was W/O emulsion.

Figure S7 Wettability of oleic acid drop on the water wetted MIL-100(Fe)

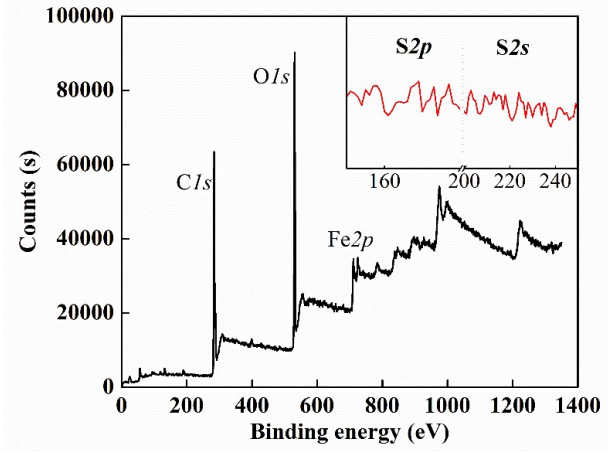

Figure S8 XPS spectra of the used MIL-100(Fe) (the inset is enlarged drawing for S*2p* and S*2s*)

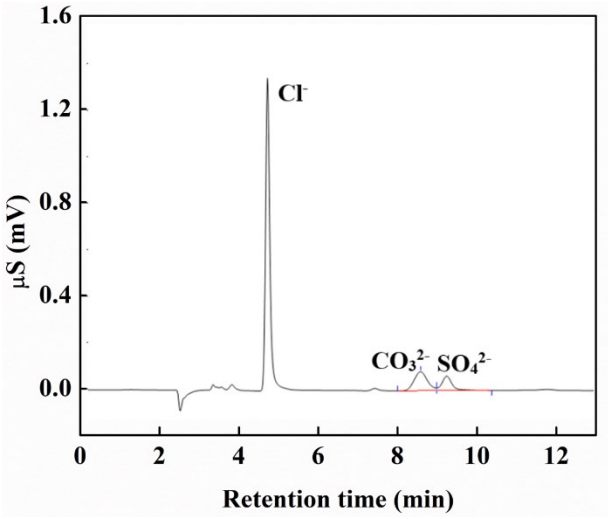

Figure S9 Ionic chromatography (IC) of SDS solution after interaction with MIL-100(Fe)

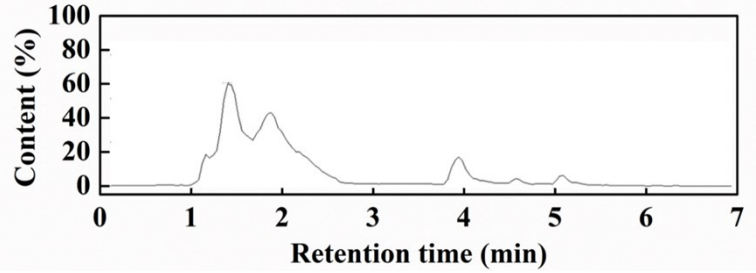

Figure S10 Liquid chromatography-mass spectrum (LC-MS) of SDS solution after interaction with MIL-100(Fe)

Figure S11 Mass spectrum of the components at 1.1 min for the LC measurement

Figure S12 Mass spectrum of the component at 4.0 min for the LC measurement

Figure S13 Mass spectrum of the components at 4.6 min for the LC measurement

Figure S14 Mass spectrum of the components at 5.1 min for the LC measurement

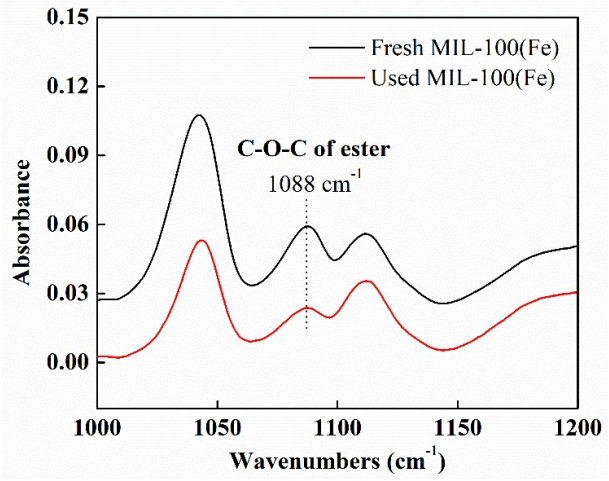

Figure S15 ATR-IR spectra for the fresh and used MIL-100(Fe) among a region of 1000~1200 cm^{-1}

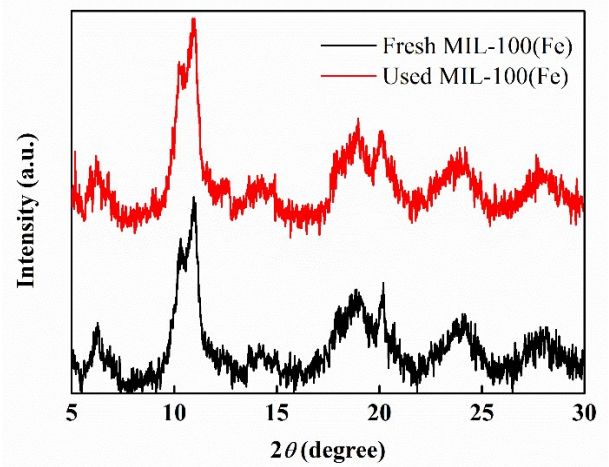

Figure S16 XRD patterns of fresh and used MIL-100(Fe)

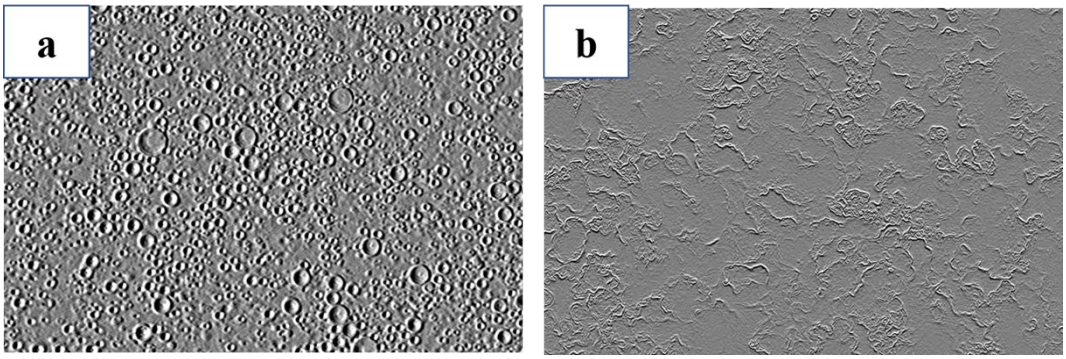

Figure S17 Margin of SDS stabilized O/W model emulsion (a) and that of demulsification using MIL-100(Fe) (b)

References

[16] A. M. Atta, H. A. Al-Lohedan and M. M. S. Abdullah, Dipoles poly(ionic liquids) based on 2-acrylamido-2-methylpropane sulfonic acid-co-hydroxyethyl methacrylate for demulsification of crude oil water emulsions, *J. Mol. Liq*., 2016, **222**, 680-690.

[18] E. A. El-Sharaky, A. E. El-Tabey and M. R. Mishrif, Novel star polymeric nonionic surfactants as crude oil emulsion breakers, *J. Surfactants Deterg*., 2019, **22**, 779-793.

[35] J. Ma, X. G. Li, X. Y. Zhang, H. Sui, L. He and S. Y. Wang, A novel oxygen-containing demulsifier for efficient breaking of water-in-oil emulsions, *Chem. Eng. J*., 2019, **385**, 123826.

[36] F. X. Feitosa, R. S. Alves and H. B. de Sant'Ana, Synthesis and application of additives based on cardanol as demulsifier for water-in-oil emulsions, *Fuel*, 2019, **245**, 21-28.

[37] F. Wang, S. W. Fang, M. Duan, Y. Xiong and X. J. Wang, Synthesis of a novel demulsifier by one-pot synthesis using two PEO-PPO demulsifiers as materials and the study of its demulsification performance, *Sep. Sci. Technol*., 2019, **54**, 1233-1240.

[38] J. Liu, X. C. Li, W. H. Jia, M. S. Ding, Y. Zhang and S. L. Ren. Separation of emulsified oil from oily wastewater by functionalized multiwalled carbon nanotubes, *J. Disper. Sci. Technol.*, 2016, **37**, 1294-1302.

[39] Y. C. Du, P. C. Si, L. Q. Wei, Y. L. Wang, Y. B. Te, G. H. Zuo, B. Yu, X. M. Zhang and S. F. Ye, Demulsification of acidic oil-in-water emulsions driven by chitosan loaded $Ti_3C_2T_x$, *Appl. Surf. Sci*., 2019, **476**, 878-885.

[40] X. H. Mao, L. Gong, L. Xie, H. Qian, X. G. Wang and H. B. Zeng, Novel Fe_3O_4 based superhydrophilic core-shell microspheres for breaking asphaltenes-stabilized water-in-oil emulsion, *Chem. Eng. J*., 2018, **358**, 869-877.